PAPER

Passive Two-dimensional Wave Digital Filters used in a Multirate System having Perfect Reconstruction

Achim GOTTSCHEBER[†], *Student Member and* Akinori NISHIHARA[†], *Member*

SUMMARY This paper is concerned with the design and implementation of a 2-channel, 2-dimensional filter bank using rectangular (analog/digital) and quincunx (digital/digital) sampling. The associated analog low-pass filters are separable where as the digital low-pass filters are non-separable for a minimum sampling density requirement. The digital low-pass filters are Butterworth type filters, $N = 9$, realized as LWDFs. They, when itterated, approximate a valid scaling function (raised-cosine scaling function). The obtained system can be used to compute a discrete wavelet transform.

key words: *orthogonal wavelet bases, wave digital filter, raised-cosine scaling function, 2-dimensional filter bank*

1. Introduction

1.1 WDF

Motivated by the fact that for a given filter specification IIR-filters have much less complexity compared to FIR-filters, this paper is concerned with the design of non-separable 2-dimensional IIR-filters by means of wave digital filters (WDFs). They are suitable for multirate systems to generate orthonormal wavelet bases. An implementation of perfect reconstruction QMF banks using IIR filters for infinite length signals was first shown in [12]. This method was modified in [13] for 1-dimensional WDFs. In this paper it is used for non-separable 2-dimensional lattice WDFs using quincunx sampling.

WDFs [4], [5], [7] are very well suited to be used in multirate digital filter arrangements and in particular for realizing filter banks [6]. They are preferably derived from lossles classical (analog) filters. Thus, one can assign an analog reference filter to every WDF. Lattice reference filters yield lattice WDFs (LWDF). They are a very attractive subclass of WDFs and especially in the bireciprocal case [9] when using real filter coefficients. Stability of an IIR-filter is in general difficult to deal with. It is closely related to passivity, especially internal passivity. WDF, when properly designed, are built up of internal passive circuits which are then automatically stable. For more details on stability related to multi-dimensional WDFs, we refere to [10] and references therein. Digital filter banks with perfect reconstruction can be build when the analysis and the synthesis filters form a paraunitary system, i.e., [13], [16] written in matrix form* $\mathbf{S}_*\mathbf{S} = \mathbf{E}$, where $\mathbf{E}$ denotes the identity matrix. If in addition each filter of $\mathbf{S}$ is stable, the scattering matrix $\mathbf{S}$ is said to be lossless. In the case of WDFs, the filters of $\mathbf{S}_*$ are unstable if the filters of $\mathbf{S}$ are stable [16]. Nevertheles, in [12], [13] it is shown how to implement the unstable filters of $\mathbf{S}_*$ in a stable way and summarized for the 1-dimensional LWDF case next.

1.2 WDF and Perfect Reconstruction

A stable realization of the filters of $\mathbf{S}_*$ is achieved in three steps. Step 1 requires to properly initialize the synthesis filters before filtering takes place.

Considering the analysis filters of a two-channel LWDF bank, polyphase representation in Fig. 1, the all-pass sections $F_i(z)$ have the special form (bireciprocal case)

$$F_i(z) = \frac{z^{-1} - \alpha_i}{1 - \alpha_i z^{-1}}. \tag{1}$$

Since the same all-pass filters are used in the analysis and synthesis QMF bank, a state-variable representation of each single all-pass section, compare Fig. 2, is useful. For the analysis side: $\mathbf{T}_a(n+1) = \mathbf{a}\mathbf{T}_a(n) + \mathbf{b}x_{in}(n)$,

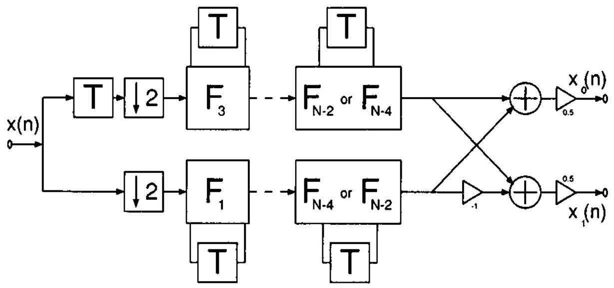

Fig. 1 Block diagram of the analysis filters of a two-channel LWDF QMF bank (bireciprocal case) for $N = 5, 9, 13, \cdots$ or $N = 7, 11, 15, \cdots$ in polyphase representation, $1/T$ the sampling rate.

*$h(n) \rightarrow h(-n) \Rightarrow H(\omega) \rightarrow H_*(\omega)$, where for a real rational function $F = F(\omega)$ the paraconjugate $F_* = F_*(\omega)$ is defined by $F_*(\omega) = F(-\omega)$. For a matrix, paraconjugation implies not only paraconjugation of each entry, but also transposition.

Manuscript received April 24, 1996.
Manuscript revised August 14, 1996.

[†]The authors are with Department of Physical Electronics, Tokyo Institute of Technology, Tokyo, 152 Japan.

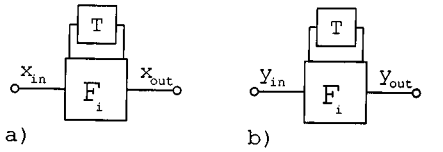

Fig. 2 All-pass section F_i: (a) analysis, (b) synthesis side.

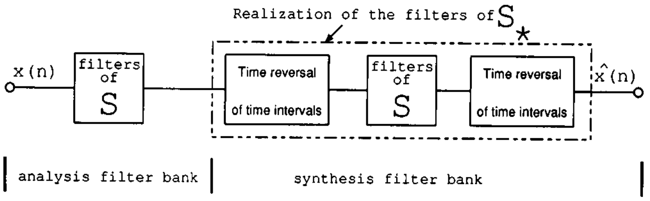

Fig. 3 System for perfect reconstruction, FIR or IIR, for infinite length signals.

$x_{out}(n) = \mathbf{c}\mathbf{T}_a(n) + \mathbf{d}x_{in}(n)$, and in the case for the synthesis side, $\mathbf{T}_a, x_{in}$ and x_{out} are replaced with $\mathbf{T}_s, y_{in}$ and y_{out}, respectively. $\mathbf{T}_a$, $\mathbf{T}_s$ denote the state-variable vectors of the analysis and synthesis side, which are related as $\mathbf{T}_s(0) = \mathbf{G}\mathbf{T}_a(P)$ by the matrix

$$\mathbf{G} = \begin{bmatrix} 0 & 1 \\ 1 & 0 \end{bmatrix}, \tag{2}$$

where $y_{out}(n) = x_{in}(P-n-1)$ for $n = 0, 1, \cdots, P-1$, P the number of samples in the time interval. Step 2 is indicated in Fig. 3, where an infinite length signal is divided in time intervals which are then fed into the filters of the synthesis filter bank in a time reversed manner. Step 3, also shown in Fig. 3, requires the time intervals to be time reversed after the filtering process and to be joined together to form the output signal $\hat{x}(n)$. Note, the time reversal of the time intervals is done in blocks. The block length is a multiple of the sampling interval T, and time reversal is simply implemented by a reversal of the relevant pointers to the samples in the blocks.

2. 2-Dimensional Nonseparable Wavelets

In the 1-dimensional case wavelet bases can be constructed from Butterworth filters[17] when used in a perfect reconstruction QMF bank. The implementation as LWDFs of those filters is very efficient[8] and will be used when constructing a nonseparable perfect reconstruction filter bank for quincunx sampling.

2.1 Paraunitary Filter Bank (LWDF)

In the 1-dimensional case, a bandlimited (by means of an analog filter $\varphi(t)$) signal $x_a(t)$ having no spectral components above f_m Hz, can be determined uniquely by values sampled at uniform intervals of T seconds where $T \leq \frac{1}{2f_m}$. In the D-dimensional case, the minimum sampling density ρ_{min} (number of lattice points per unit hypervolume) is defined as[3]

$$\rho_{min} = \frac{1}{\mid det\mathbf{V} \mid}, \tag{3}$$

where $\mathbf{V}$ is the sampling matrix used when sampling bandlimited signals. The minimum sampling density ρ_{min} depends on $\mathbf{V}$ and on the support of the bandlimited signal. The support of the bandlimited signal is determined by the shape of $\varphi(\mathbf{t})$.

In a 1-dimensional multirate system, a signal $x(n)$, bandlimited to the region $\mid \omega \mid < \frac{\pi}{C}$ (by means of a digital filter $h_0(n)$, C = number of channels), can be alias-free downsampled. In the D-dimensional case, alias-free downsampling is directly related to the matrix $\mathbf{M}$. The decimation ratio r is defined as $r = \mid det\mathbf{M} \mid$. In the case that an orthonormal wavelet transform is performed by means of a multirate system, the analog filter $\varphi(t)$ and the digital filter $h_0(n)$ are related in frequency domain as[1],[2] $\Phi(\omega) = \prod_{k=1}^{\infty} M_0(j2^{-k}\omega)$, where $M_0(\omega) = H_0(e^{j\omega})/H_0(0)$. The ideal filter $H_0(e^{j\boldsymbol{\omega}})$ in a D-dimensional multirate filter design has the form

$$H_0(e^{j\boldsymbol{\omega}}) = \begin{cases} 1 & \text{if } \boldsymbol{\omega} = \pi\mathbf{M}^{-T}\mathbf{x} + 2\pi\mathbf{m}, \\ & \text{for some } \mathbf{x} \in [-1,1)^D, \mathbf{m} \in N \\ 0 & \text{elsewhere} \end{cases} \tag{4}$$

where $\boldsymbol{\omega} = [\omega_0 \ \omega_1 \ \cdots \ \omega_{D-1}]^T$, $\mathbf{M}$ is a $D \times D$ nonsingular matrix, M^{-T} stands for $(M^{-1})^T$ and $2\pi\mathbf{m}$ represents the periodicity.

The analog and digital low-pass filters are then related as[2],[14],[15]

$$\Phi(\boldsymbol{\omega}) = \prod_{k=1}^{\infty} M_0(j\mathbf{M}^{-k}\boldsymbol{\omega}) \tag{5}$$

where $M_0(\boldsymbol{\omega}) = H_0(e^{j\boldsymbol{\omega}})/H_0(\mathbf{0})$. As $\mathbf{M}$ in (5) determines the shape of $\varphi(\mathbf{t})$, it follows that $\mathbf{V}$ in (3) is related to $\mathbf{M}$.

Note, that $\varphi(\mathbf{t})$ must be an analog filter having compact support in frequency domain in order to be able to uniquely reconstruct, by means of an interpolation formula, an analog signal from its discretely represented signal. This means that the associated digital low-pass filter $h_0(\mathbf{n})$ has in general an infinite number of nonzero filter coefficients and can therefore not excactly be realized. However, in the following an exact realizable $h_0(\mathbf{n})$ (2-dimensional case) will be designed for a perfect reconstruction system having a finite number of non-zero filter coefficients, that yield an $\varphi(t)$ which has infinite support in frequency domain.

Considering the 2-dimensional non-separable case, one choice of $\mathbf{M}$ for quincunx sampling is (symmetry dilation matrix)

$$\mathbf{M}_q = \begin{bmatrix} 1 & 1 \\ 1 & -1 \end{bmatrix}. \tag{6}$$

$\mathbf{M}_q$ is said to be well behaved[14]. Based on $\mathbf{M}_q$, 2-dimensional nonseparable wavelets will be derived.

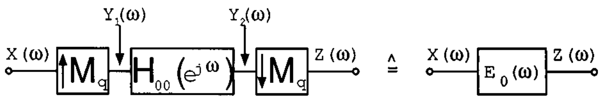

Fig. 4 0th Type 1 polyphase component of $H_{00}(e^{j\boldsymbol{\omega}})$.

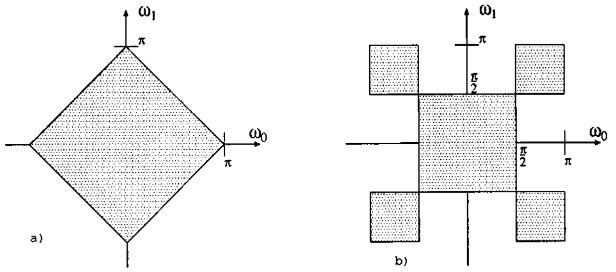

Fig. 5 (a) Ideal digital low-pass filter shape $E_0(\boldsymbol{\omega}) = H_0(e^{j\boldsymbol{\omega}})$ for quincunx sampling with $\mathbf{M}_q$, (b) $H_{00}(e^{j\boldsymbol{\omega}})$. The dotted areas indicate the pass-band of the filters.

Figure 4 shows the 0th Type 1 polyphase component [6], [18]–[20] of $H_{00}(e^{j\boldsymbol{\omega}})$. Assuming $H_{00}(e^{j\boldsymbol{\omega}}) = H_L(e^{j\omega_0})H_L(e^{j\omega_1}) + H_H(e^{j\omega_0})H_H(e^{j\omega_1})$ and using the transforms

$$Y_1(\boldsymbol{\omega}) = X(\mathbf{M}^T\boldsymbol{\omega}) \tag{7}$$

and

$$Z(\boldsymbol{\omega}) = \frac{1}{\mid det\mathbf{M} \mid} \sum_{\mathbf{k}\in N(\mathbf{M}^T)} Y_2(\mathbf{M}^{-T}(\boldsymbol{\omega} - 2\pi\mathbf{k})), \tag{8}$$

representing upsampling and downsampling respectively, $\mathbf{k}$ the set of integer vectors inside the fundamental parallelepiped, it turns out that $E_0(\boldsymbol{\omega})$ equals the ideal low-pass filter $H_0(e^{j\boldsymbol{\omega}})$ associated to the quincunx sampling matrix $\mathbf{M}_q$. Compare Fig. 5 for a proper choice of $H_{00}(e^{j\boldsymbol{\omega}})$. This way of realizing $H_0(e^{j\boldsymbol{\omega}})$ is very attractive as will be seen later. A pictorial proof that $E_0(\boldsymbol{\omega})$ indeed represents $H_0(e^{j\boldsymbol{\omega}})$ is illustrated in Fig. 6. In general, when upsampling/downsampling with $\mathbf{M}$, the lattice is squeezed/streched by $\mid det\mathbf{M} \mid$ and after downsampling $\mathbf{M}$ also renumbers the lattice points. Concrete, the input lattice $\mathbf{V}$, written in frequency domain as

$$\mathbf{U} = 2\pi\mathbf{V}^{-T} = 2\pi \begin{bmatrix} 1 & 0 \\ 0 & 1 \end{bmatrix}$$

and shown in Fig. 6 (a), undergoes an interpolation with $\mathbf{M}_q$ by (7). This results in the lattice which is illustrated in Fig. 6 (b). Figure 6 (b) also shows one period of $H_{00}(e^{j\boldsymbol{\omega}})$. Downsampling with (8) finally gives back the desired input lattice filtered by the ideal low-pass filter $H_0(e^{j\boldsymbol{\omega}})$, where only one period of $H_0(e^{j\boldsymbol{\omega}})$ is depicted. If $H_L(e^{j\omega_0}) = 0$ and $H_L(e^{j\omega_1}) = 0$ at $\omega_0 = \pi$ and $\omega_1 = \pi$, respectively, then $H_0(e^{j\boldsymbol{\omega}}) = \mathbf{0}$ at $\boldsymbol{\omega} = (\pi, \pi)$. Similarly one can design a high-pass filter $H_{01}(e^{j\boldsymbol{\omega}}) = H_H(e^{j\omega_0})H_L(e^{j\omega_1}) + H_L(e^{j\omega_0})H_H(e^{j\omega_1})$, see Fig. 7. Since $\mathbf{M}_q\mathbf{M}_q = \mathbf{M}_{rec}$,

$$\mathbf{M}_{rec} = \begin{bmatrix} 2 & 0 \\ 0 & 2 \end{bmatrix} \tag{9}$$

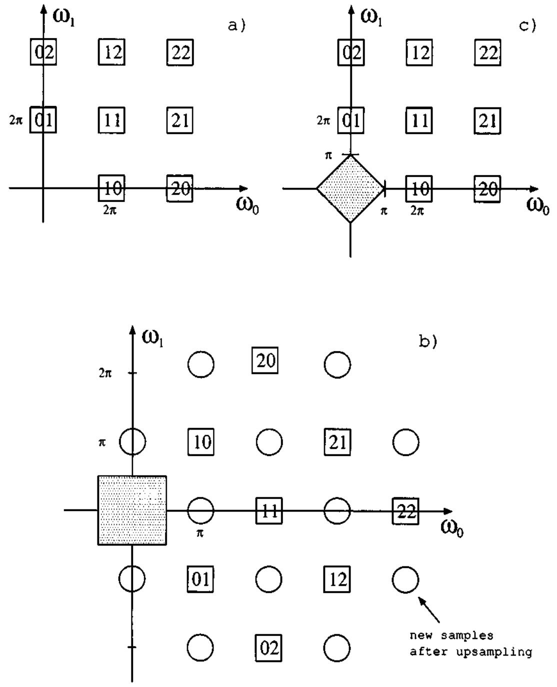

Fig. 6 Lattice reprensentations in frequency domain, (a) input lattice, (b) after upsampling with $\mathbf{M}_q^T$, $H_{00}(e^{j\boldsymbol{\omega}})$ is indicated, and (c) after downsampling with $\mathbf{M}_q^{-T}$.

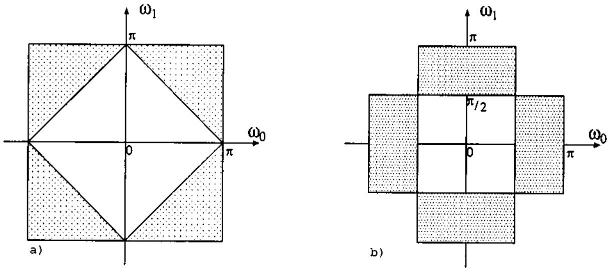

Fig. 7 (a) Ideal digital high-pass filter shape $H_1(e^{j\boldsymbol{\omega}})$ for quincunx sampling with $\mathbf{M}_q$, (b) $H_{01}(e^{j\boldsymbol{\omega}})$.

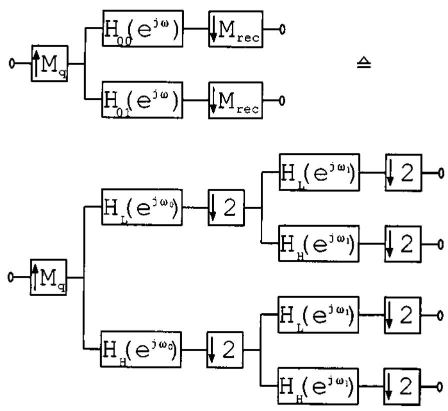

Fig. 8 Efficient structure for a 2-dimensional nonseparable perfect reconstruction filter bank with quincunx sampling (analysis part).

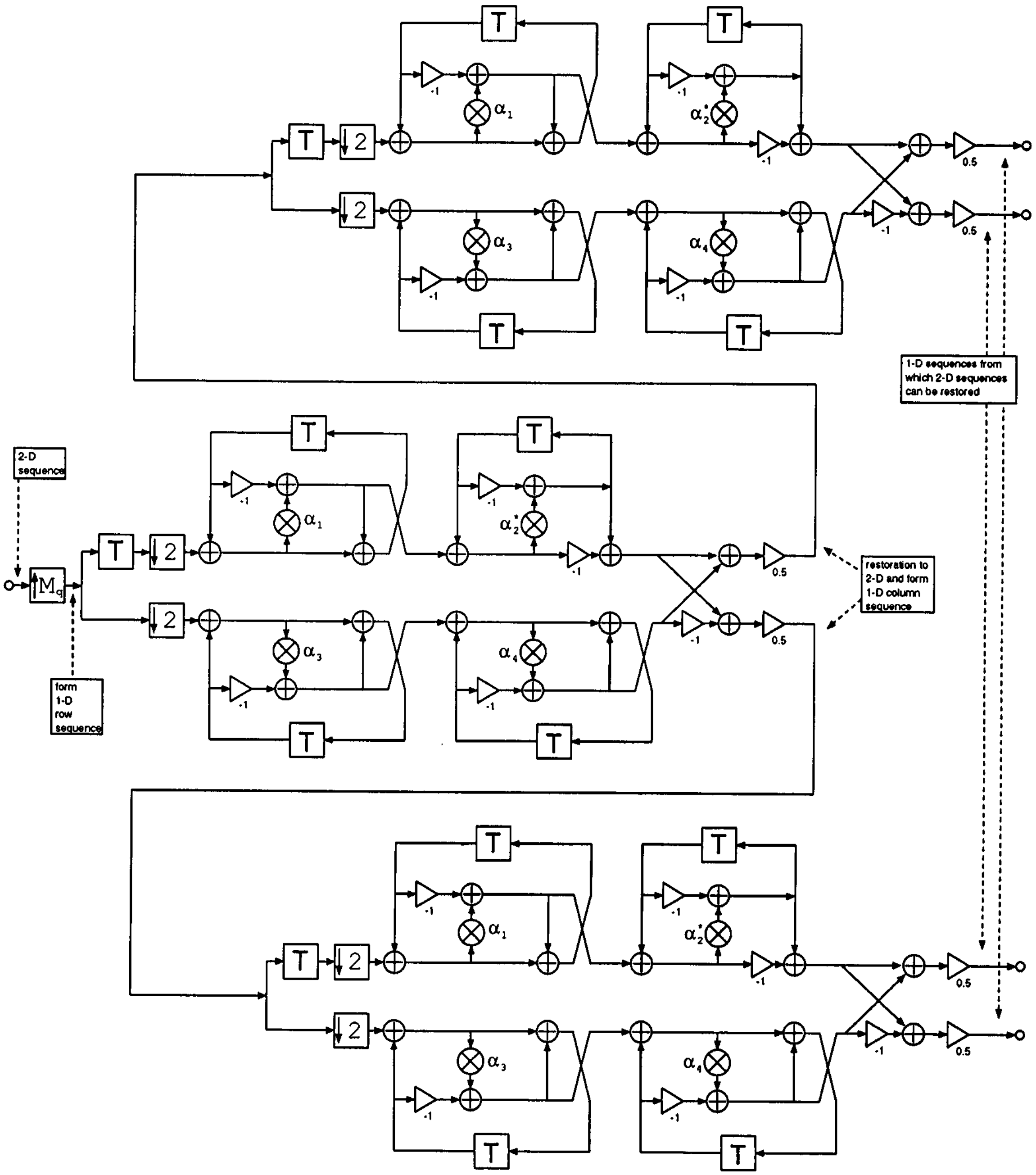

Fig. 9 2-dimensional, 2-channel nonseparable LWDF bank (analysis part) for quincunx downsampling, expressed in an internal separable way.

the 2-dimensional nonseparable QMF bank, using $\mathbf{M}_q$, can be implemented with separable filters. And when realized with LWDF this structure becomes very simple. The designed perfect reconstruction filter bank can be used to perform a non-separable 2-dimensional wavelet transform. Clearly, the final structure representing a 2-dimensional nonseparable perfect reconstruction filter bank with quincunx sampling is shown in Fig. 8. This structure can be applied for FIR and IIR filters. It can be very efficiently implemented, especially in the bireciprocal LWDF case. Figure 9 shows an example for a Butterworth implementation of a LWDF, $N = 9$, maximum number of zeros at $\omega = (\pi, \pi)$. This structure uses 12 filter coefficients (only 4 of them beeing different) and they can be calculated with a pocket calculator by using the method shown in [8]. Filter coefficients used in Fig. 9:

$$\alpha_1 = -0.132\,47$$
$$\alpha_2^* = 0.295\,91$$
$$\alpha_3 = -0.031\,09$$
$$\alpha_4 = -0.333\,33$$

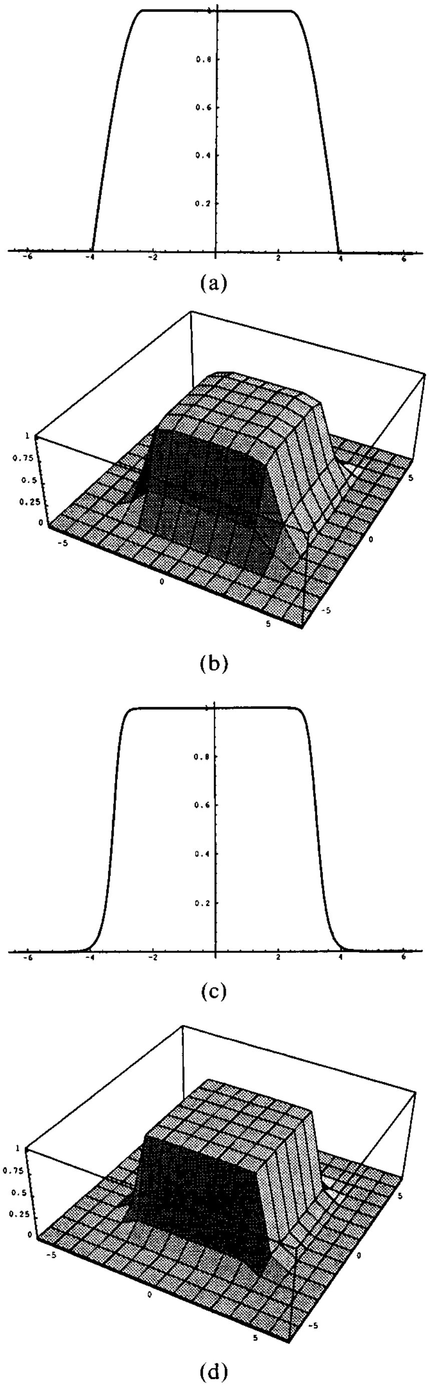

Fig. 10 Frequency responses of the raised-cosine scaling function, with $\alpha = 0.25$, and the itterated WDF, $N = 9$; (a) and (c) show the 1-dimensional frequency responses, (b) and (d) show the 2-dimensional frequency responses of the filters, respectively.

Note, $N = 9$ was chosen because this choice for realizing $H_0(e^{j\boldsymbol{\omega}})$, when used in Eq. (5), will result in a good approximation for the associated raised-cosine scaling function having a roll-off factor of $\alpha = 0.25$ [11]. Compare Fig. 10. With $\alpha_2 = -(1-\alpha_2^*)$, the 1-dimensional frequency response of $H_L(e^{j\omega_0})$ follows as

$$H_L(e^{j\omega_0}) = 0.5\left(e^{j\omega_0}\frac{e^{j2\omega_0}-\alpha_1}{1-\alpha_1 e^{j2\omega_0}}\frac{e^{j2\omega_0}-\alpha_2}{1-\alpha_2 e^{j2\omega_0}} + \frac{e^{j2\omega_0}-\alpha_3}{1-\alpha_3 e^{j2\omega_0}}\frac{e^{j2\omega_0}-\alpha_4}{1-\alpha_4 e^{j2\omega_0}}\right)$$

2.2 Constructing 2-D Wavelet Bases from LWDFs

In general the number of wavelets is determined by

$$|\,det(\mathbf{M})\,| - 1 = r - 1. \qquad (10)$$

Unlike the separable case, $\mathbf{M}_{rec}$, in which three mother wavelets ψ_1, ψ_2, ψ_3 and one scaling function φ exists, in the quincunx case, $\mathbf{M}_q$, there exists only one mother wavelet ψ and one scaling function φ [2], [15]. The corresponding itterated filter bank for quincunx $\mathbf{M}_q$, representing the scaling function and wavelet, is indicated in Fig. 11. And Fig. 12 shows various dilated versions of the ideal basic filters for $\mathbf{M}_q$, which take part in the infinite products of (5) and

$$\Psi(\boldsymbol{\omega}) = M_1(j\mathbf{M}^{-1}\omega)\Pi_{k=2}^{\infty}M_0(j\mathbf{M}^{-k}\omega) \qquad (11)$$

where $M_1(j\boldsymbol{\omega}) = H_1(e^{j\boldsymbol{\omega}})/H_1(\mathbf{0})$. For $\mathbf{M}_q$ the scaling function φ is separable in the sense that it can be expressed directly in terms of one dimensional functions, i.e.,

$$\Phi_q(\boldsymbol{\omega}) = \Phi(\omega_0)\Phi(\omega_1) \qquad (12)$$

or in time domain as

$$\varphi_q(\mathbf{t}) = \varphi(t_0)\varphi(t_1). \qquad (13)$$

The wavelet follows as:

$$\Psi_q(\boldsymbol{\omega}) = \Phi_q(\mathbf{M}^{-1}\boldsymbol{\omega})M_1(j\mathbf{M}^{-1}\boldsymbol{\omega}). \qquad (14)$$

3. Discussions

3.1 Minimum Sampling Density for V Related to $\mathbf{M}_q$

Since the shape of $\varphi(t)$ determines indirectly ρ_{min}, the (analog/digital) sampling matrix $\mathbf{V}$ for (3) is derived from the (digital/digital) sampling matrix $\mathbf{M}_q$. For $x(\mathbf{n}) = x_a(\mathbf{Vn})$ and with $\boldsymbol{\Omega} = \mathbf{V}^T\boldsymbol{\omega}$ it follows

$$X(\mathbf{V}^T\boldsymbol{\Omega}) = \frac{1}{|\,det(\mathbf{V})\,|}\sum_{\mathbf{k}\in N} X_a(j(\boldsymbol{\Omega}-\mathbf{Uk})). \qquad (15)$$

It is clear from Fig. 13, that $\mathbf{V}$ has for ρ_{min} (tightest packed $X(\mathbf{V}^T\boldsymbol{\Omega})$) the form

$$\mathbf{V} = \begin{bmatrix} v_0 & 0 \\ 0 & v_1 \end{bmatrix} \qquad (16)$$

or in frequency domain

$$\mathbf{U} = 2\pi\mathbf{V}^{-T} = 2\pi\begin{bmatrix} v_0^{-1} & 0 \\ 0 & v_1^{-1} \end{bmatrix} \qquad (17)$$

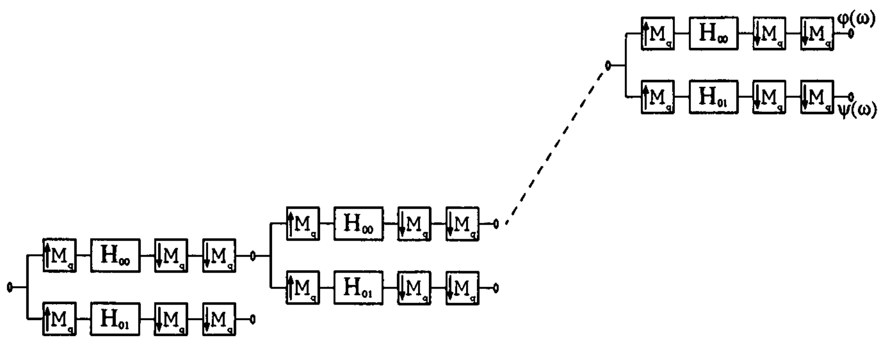

Fig. 11 Computation of the 2-dimensional discrete wavelet transform using a filter bank with quincunx sampling.

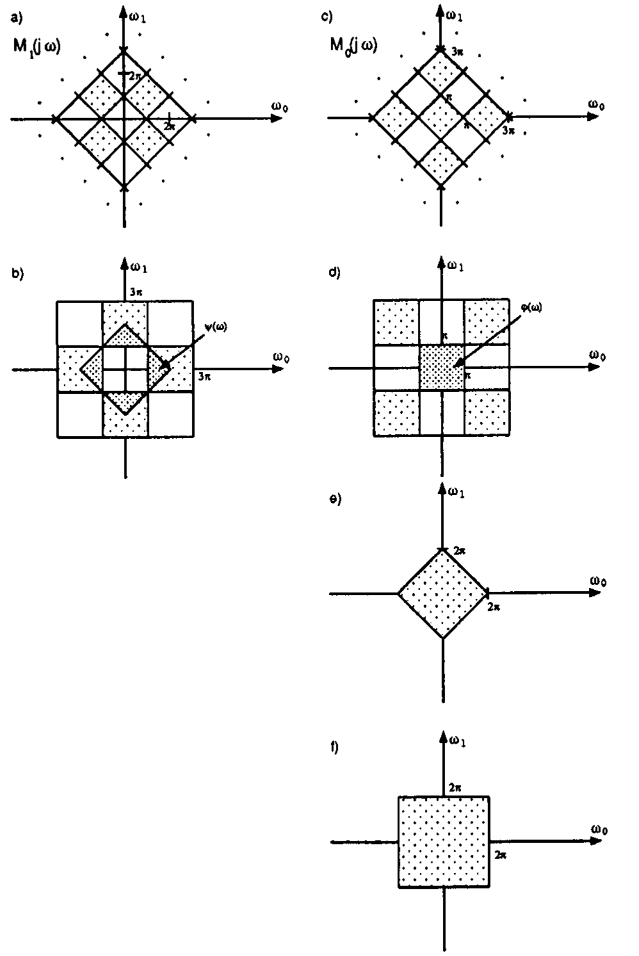

Fig. 12 Various dilated versions of the ideal basic filters shown in (a) and (c) which take part in the infinite product (b), (d), (e) and (f). In (b) and (d), the wavelet and scaling function are indicated, respectively.

And aliasing can be avoided for the values

$$v_0 = 1$$
$$v_1 = 1.$$

Thus $\rho_{min} = 1$. It can be easily shown that the arrangement in Fig. 13 (c) yields also $\rho_{min} = 1$.

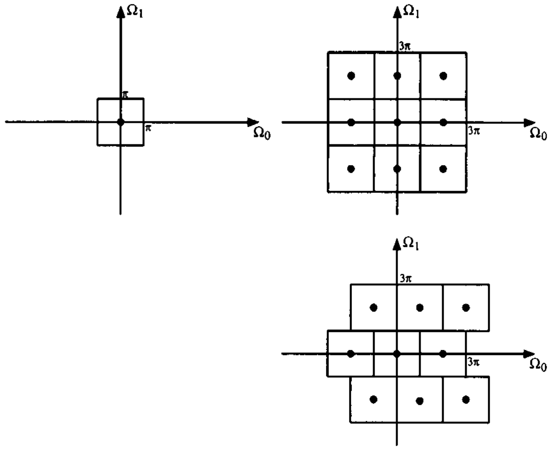

Fig. 13 Ideal (analog/digital) sampling with $\mathbf{V}$ for (digital/digital) quincunx sampling with $\mathbf{M}_q$. (a) Support of $X_a(j\boldsymbol{\Omega})$, (b) support of $X_a(\mathbf{V}^T\boldsymbol{\Omega})$, rectangular sampling, (c) alternative choice for $\mathbf{V}$.

3.2 Compact Support in Frequency Domain

The unavoidable error caused by discretisation of an continuous function is responsible for the following approximation and is in particular due to (5) and $x(\mathbf{n}) = \int x(\mathbf{t})\varphi(\mathbf{t}-\mathbf{n})dt$.

As mentioned above, $h_0(\mathbf{n})$ was designed as a LWDF (Butterworth filter, $N = 9$) whose associated analog low-pass filter $\Phi(\boldsymbol{\omega})$ in (5) has not compact support. It is thus an approximation to a "valid" scaling function ($\Phi(\boldsymbol{\omega})$ with compact support). Our choice for the valid scaling function was the raised-cosine scaling function [11] with $\alpha = 0.25$, that, when approximated, leads to a fairly good overall system performance. From our experience, the two extremes of the raised-cosine scaling function, namely (a) the sinc scaling function ($\alpha = 0$) and (b) a Meyer scaling function ($\alpha = \frac{1}{3}$), are not the best choice for a valid scaling function since (a) requires a too large filter degree N and (b) too many samples per hypervolume. However, the precise relationship for a "best" approximation in this sense remains as future work.

Note, that for the same filter specification a 1-dimensional FIR-filter requires $N = 49$. Thus an IIR-filter results in a better performance and when implemented as a LWDF, only 4 multipliers are necessary which operate at a lower sampling rate due to a polyphse decomposition.

4. Conclusions

The blockdiagram of Fig. 1 as well as Fig. 3 are used in connection with the method illustrated in Fig. 4 and Fig. 8 to design and implement a perfect reconstruction filter bank with LWDFs. This system computes a 2-dimensional discrete wavelet transform illustrated in Fig. 11. And it has a minimum sampling density ρ_{min} for the ideal filters associated to $\mathbf{V}$ and $\mathbf{M}_q$ depicted in Figs. 12 and 13, respectively.

5. Acknowledgement

The first author would like to express his gratitude to Professor emeritus Dr. sc. techn., Dr. h.c. mult. Alfred Fettweis for many interesting teachings received in the early state of this paper during a three months visit at Ruhr-Universitaet Bochum.

References

[1] N. Fliege, "Multirate Digital Signal Processing," John Wiley & Sons, 1994.
[2] M. Vetterli and J. Kovacevic, "Wavelets and subband coding," Prentice Hall, Englewood Cliffs, 1995.
[3] P.P. Vaidyanathan, "Multirate Systems and Filter Banks," Prentice Hall, Englewood Cliffs, 1993.
[4] A. Fettweis, "Wave digital filters: Theory and praxis," Proc. IEEE, vol.74, no.2, pp.270–327, Feb. 1986.
[5] A. Fettweis, "Digital circuits and systems," IEEE Trans. Circuits & Syst., vol.CAS-31, no.1, Jan. 1984.
[6] A. Fettweis, T. Leickel, M. Bolle, and U. Sauvagerd, "Realization of Filter banks by means of wave digital filters," IEEE Int. Symp. on Circuits and Systems, 1990.
[7] A. Fettweis, "Digital filter structures related to classical filter networks," Arch. Elektr. Uebertragung, vol.25, no.2, pp.79–89, Feb. 1971.
[8] L. Gaszi, "Explicit formulae for lattice wave digital filters," IEEE Trans., vol.CAS-32, pp.68–88, Jan. 1985.
[9] A. Nossek and H.D. Schwarz, "Wave digital lattice filters with applications in communication systems," Proc. IEEE Int. Symp. Circuits and Systems, pp.845–848, May 1983.
[10] G. Hemetsberger, "Numerische integration hyperbolischer partieller differentialgleichungen unter verwendung mehrdimensionaler wellendigitalfilter," Doctoral dissertation, Ruhr-Univ. Bochum, 1995.
[11] A. Gottscheber and A. Nishihara, "Wavelet bases derived from the raised-cosine filter," IEICE Trans. on Fundamentals, vol.E80-A, no.1 pp.126–132, Jan. 1997.
[12] S.K. Mitra, C. Creusere, and H. Babic, "A novel implementation of perfect reconstruction QMF banks using IIR filters for infinite length signals," IEEE Int. Symp. on Circuits and Systems, pp.2312–2315, 1992.
[13] T. Leickel, "Entwurf und realisierung diskreter filterbaenke," Doctoral dissertation, Ruhr-Univ. Bochum, 1994.
[14] J. Kovacevic and M. Vetterli, "Nonseparable multidimensional perfect reconstruction filter banks and wavelet bases for R^n," IEEE Trans. Inf. Theory, vol.38, no.2, March 1992.
[15] A. Cohen and I. Daubechies, "Nonseparable bidimensional wavelet bases," Rev. Mat. Iberoamericana, vol.9, no.1, pp.51–137, 1993.
[16] A. Fettweis, J. A. Nossek, and K. Meerkoetter, "Reconstruction of signals after filtering and sampling rate reduction," IEEE Trans. Acoust., Speech & Signal Process., vol.ASSP-33, no.4, Aug. 1985.
[17] C. Herley and M. Vetterli, "Wavelets and recursive filter banks," IEEE Trans. Signal Proc., vol.41, no.8, pp.2536–2556, Aug. 1993.
[18] R.M. Merserau and T.C. Speake, "The processing of periodically sampled multidimensional signals," IEEE Trans. Acoust., Speech & Signal Process., vol.ASSP-31, pp.188–194, Feb. 1983.
[19] G. Linnenberg, "Ueber die discrete verarbeitung mehrdimensionaler signale unter verwendung von wellendigitalfiltern," Doctoral dissertation, Ruhr-Univ. Bochum, 1984.
[20] T. Chen and P.P. Vaidyanathan, "Multidimensional multirate filters derived from one dimensional filters," Electron. Lett., vol.27, pp.225–228, Jan. 1991.

Achim Gottscheber was born in Bad Wimpfen, Germany, on January 1, 1965. He received the Dipl.-Ing. (FH) degree from the Fachhochschule Aalen, Aalen, Germany, 1992 and the M.Sc. degree from the University of London, King's College, London, UK, 1993. He is currently a Ph.D. student at Tokyo Institute of Technology in the Department of Physical Electronics. His research interests include digital signal processing and digital communication theory. Mr.Gottscheber is a student member of IEEE.

Akinori Nishihara was born in Fukuoka, Japan on February 26, 1951. He received the B.E., M.E. and Dr.Eng. degrees in electronics from Tokyo Institute of Technology in 1973, 1975 and 1978, respectively. Since 1978 he has been with Tokyo Institute of Technology, where he is now Professor of the Center for Research and Development of Educational Technology. His main research interests are in filter design, 1D and multi-D signal processing, and modern applications of classical circuit theory. From 1990 to 1994 he served as an Associate Editor of the IEICE Trans. Fundamentals, and is now serving as an Associate Editor of the IEEE Trans. Circuits and Systems II. He was Student Activities Committee Chair, IEEE Region 10 (Asia Pacific Region) for 1995–1996. Dr. Nishihara is a member of IEEE, EURASIP, ECS and JET.